



# Electrical conductivity and tribological behavior of an automatic transmission fluid additised with a phosphonium-based ionic liquid



A. García Tuero<sup>a</sup>, C. Sanjurjo<sup>a</sup>, N. Rivera<sup>b</sup>, J.L. Viesca<sup>a,\*</sup>, R. González<sup>b</sup>, A. Hernández Battez<sup>a</sup>

<sup>a</sup> Department of Construction and Manufacturing Engineering, University of Oviedo, Pedro Puig Adam s/n, 33203 Gijón, Spain

<sup>b</sup> Department of Marine Science and Technology, University of Oviedo, Blasco de Garay, s/n, 33203 Gijón, Spain

## ARTICLE INFO

### Article history:

Received 14 July 2022

Revised 22 September 2022

Accepted 8 October 2022

Available online 15 October 2022

### Keywords:

Automatic transmission fluid

Electrical conductivity

Electric vehicles

Ionic liquid

Tribology

## ABSTRACT

There are electric vehicle configurations with the electric motor (EM) inside the transmission housing, putting in contact the automatic transmission fluid (ATF) with the EM. In this case the ATF must fulfil several requirements, such as electrical and material compatibilities, improved cooling performance, etc. The use of ionic liquids (IL) as lubricant additive can impact on electrical conductivity ( $\kappa$ ) and tribological behaviour of the ATF. This work analyses the influence of a phosphonium-based ionic liquid ([P<sub>6,6,6,14</sub>][BEHP]) used as additive at 1 and 3 wt% concentration on the abovementioned properties of a commercial ATF. The addition of the IL increased the  $\kappa$  of the ATF but it continues being dissipative; however, the dielectric strength decreased drastically and further tests about this property should be performed. The IL promotes the formation of a phosphorous-rich tribofilm, which is related to the improved antiwear performance. This formulation including the IL could be used in electric vehicles.

© 2022 The Author(s). Published by Elsevier B.V. This is an open access article under the CC BY-NC license (<http://creativecommons.org/licenses/by-nc/4.0/>).

## 1. Introduction

The electric vehicle (EV) is currently one of the global megatrends due to the possibility of reducing the greenhouse gases emissions. This emissions reduction, in particular CO<sub>2</sub>, is close related to the high efficiency of these vehicles [1]. Four EV types can be found in the market: mild hybrid, full hybrid, plug-hybrid and full EV. This classification is used taking into account the size and the charging mode of the battery, and the size of the electric motor (EM) used [2]. Among the hybrid electric vehicles (HEV), there are configurations where the EM and the ATF are in contact because the former is inside the transmission housing. This fact requires that the ATF fulfils numerous requirements. These requirements are: corrosion protection, magnetic compatibility, thermal compatibility, avoiding of aeration and foaming at high speeds, material compatibility, and electrical compatibility [3,4].

For achieving the abovementioned requirements, it is very important to do a proper selection of base oils and additives, and their concentration, for the formulation of the ATFs. Gao et al. [5] described a lubricating oil for electric and hybrid vehicles, which is composed by at least 80 wt% of a base oil and the rest of additives (e.g. detergent, antioxidant, antiwear, corrosion inhibitor, viscosity modifier, dispersant, etc.). The proposed lubricating oils

should have an  $\kappa$  at room temperature in the range 3000–20000 pS/m and a kinematic viscosity at 100 °C from 2 to 20 mm<sup>2</sup>/s. The use of promoters and inhibitors of conductivity has to be balanced for controlling the  $\kappa$  in low viscosity ATFs.

The ILs have been studied in lubrication since 2001 [6], mainly as an additive to a base oil, and currently continues being a hot topic of research [7–10]. Qu et al. [11] compared the most common antiwear additive (zinc dialkyldithiophosphate or ZDDP) and the ionic liquid trihexyltetradecylphosphonium bis(2-ethylhexyl)phosphate ([P<sub>6,6,6,14</sub>][DEHP] or [P<sub>6,6,6,14</sub>][BEHP]) as additive in a polyalphaolefin (PAO 4). The concentration of both compounds was limited to 1 wt% in order to fulfil the automotive engine oil specification GF 5, which limits the phosphorous content to 0.8 wt%. The IL outperformed the ZDDP at 100 °C effectively preventing the scuffing damage. On the other hand, the ionic liquid tetraoctylphosphonium bis(2-ethylhexyl)phosphate ([P<sub>8,8,8,8</sub>][DEHP]) and ZDDP were used alone and in combination as additive, limiting the phosphorous content to 0.8 wt%, and the results showed that the reduction of friction and wear was higher when the ZDDP + IL was used [12]. Similar results were obtained when the ionic liquid [P<sub>6,6,6,14</sub>][DEHP] was used with the same approach [10]. The [P<sub>6,6,6,14</sub>][DEHP] was also used as additive in fully-formulated engine oil (5 W-30) and its compatibility with the ZDDP-containing additive package was investigated [13]. While the wear rates decreased approximately 70 %, small changes were detected in friction values, which means a IL-antiwear package

\* Corresponding author.

E-mail address: [viescajose@uniovi.es](mailto:viescajose@uniovi.es) (J.L. Viesca).

synergistic effect. The use of ILs as additive in fully-formulated wind turbine gearbox oils were also studied resulting in wear reductions [14] and in lower torque loss in rolling bearing tests and lower power loss in FZG tests [15].

The use of ILs is reported as potential additives that can be included in the formulation of ATF for EVs in a preferred concentration of 0.1–5 wt% [5]. Flores-Torres et al. [16] reported the ILs as conductivity agents due to their polar nature and the capacity to increase the  $\kappa$  of a lubricating or working fluid by a tangible quantity (e.g. +100 pS/m or more). So, the ILs can be used for adjusting the  $\kappa$  of the lubricant, and there are numerous suitable cations (e.g. phosphonium, imidazolium, pyrrolidinium, etc.) that may be combined with different anions to be used with this purpose. In addition, some other additives used in the ATF's formulation, such as dispersant, detergent and antiwear (ZDDP) additives are also considered as conductivity agents. Taking into account the above facts, the inclusion of the ILs as additive in the formulation of ATF for EVs has to consider the potential changes in the  $\kappa$  of the lubricating oil in order to avoid a change from dissipative to conductive behavior under their operation temperature range and during their lifetime.

Despite the abovementioned facts, the use of ILs as additive in ATF to be used in EVs and their simultaneous implications on tribological and  $\kappa$  behaviors have not been reported. This work aims to analyze the influence of the use of the [P<sub>6,6,6,14</sub>][BEHP] ionic liquid as additive at 1 and 3 wt% in a fully-formulated ATF on the  $\kappa$  and the tribological behavior.

## 2. Experimental details

### 2.1. Materials

A commercial automatic transmission fluid (ATF) was used as reference oil and its properties are listed in Table 1. This ATF was formulated with 89 wt% of a base fluid composed by two mineral oils (YUBASE 3 and YUBASE 6) from API Group III and 11 wt% of the HiTEC 3460 additive package. The trihexyltetradecylphosphonium bis(2-ethylhexyl)phosphate ([P<sub>6,6,6,14</sub>][BEHP]) IL was provided by IOLITEC GmbH (Table 2) and included as a supplementary additive to the ATF at concentrations of 1 and 3 wt%, reducing the additive package concentration in the same ratio and keeping the total additive concentration at 11 wt% in all lubricant samples. The mixture of the ATF and the ionic liquid was prepared by using a planetary centrifugal mixer (Kakuhunter SK-300 SII) for 30 min at 1600 rpm.

### 2.2. Measurements of viscosity and electrical properties

The dynamic viscosity of the three lubricant samples was measured in a Stabinger SVM 3001 viscometer. This equipment has a kinematic viscosity measurement range from 0.2 to 30000 mm<sup>2</sup>/s, and a density measurement range from 0 to 3 g/cm<sup>3</sup>. The repeatability is 0.1 % for viscosity and 0.00005 g/cm<sup>3</sup> for density.

**Table 1**  
Properties and additive elements of the automatic transmission fluid.

Properties		Additive elements	
Density at 15 °C (g/cm <sup>3</sup> )	0.847	Ca (ppm)	–
Kinematic Viscosity at 40 °C (mm <sup>2</sup> /s)	29.8	B (ppm)	59–88
Kinematic Viscosity at 100 °C (mm <sup>2</sup> /s)	5.8	P (ppm)	136–194
Viscosity Index (VI)	144	Zn (ppm)	20
Flash Point (°C)	216	S (%)	0.192
Pour Point (°C)	–49	N (%)	–

The  $\kappa$  of the abovementioned lubricant samples was measured from 45 to 125 °C. In this case, a Digital Conductivity Meter (Emcee Model 1153) was used. The measurement range of the conductivity meter goes from 1 to 10<sup>7</sup> pS/m and at least three  $\kappa$  measurements were performed for each lubricant sample to ensure a typical deviation lower than 10 %. The temperature range for measuring electrical conductivity was selected considering the potential temperatures that gears and main parts of the EM can reach inside the transmission. These potential temperatures, related to the location of the EM inside the transmission, have been reported in a recent work [17].

The dielectric strength (breakdown voltage) was measured according to the EN 60156 standard. The test was made at room temperature (25 °C) using VDE electrodes at a distance of 2.5 mm and the voltage was increased at 2 kV/s ± 0.2 kV/s. The uncertainty of the equipment (at a confidence level of 95 %) is 4.3 kV. The lubricant sample volume was around 400 mL and it was mechanically agitated.

### 2.3. Tribological tests

In order to study friction behaviour of all lubricant samples, two different tests were performed in a Mini Traction Machine-MTM2 tribometer (PCS Instruments). Firstly, the so-called Stribeck curve were obtained through a sliding/rolling tests with the following test conditions: entrainment speed from 2500 to 10 mm s<sup>-1</sup>, load of 25 N (maximum contact pressure: 0.9 GPa), slide-to-roll ratio (SRR) of 100 % and temperatures of 40, 60, 80 and 100 °C. Secondly, traction tests were performed under the same values of load and temperature than the Stribeck curve tests, at an entrainment speed of 2000 mm s<sup>-1</sup>, load of 25 N and SRR values from 0 to 100 %. The entrainment speed and the SRR are defined by Eqs. (1) and (2), respectively. The  $u_{ball}$  and the  $u_{disc}$  are the tangential speed of the ball and the disc at the point of contact, respectively. The lubricant volume used for both tests was 10 mL. The balls (9.525 mm-radius, hardness of 800–920 HV<sub>30</sub>) and discs (hardness of 720–780 HV<sub>30</sub>) used in these tests are manufactured from AISI 52100 steel and has a surface roughness less than 0.020 μm.

$$Vs = u_{disc} - u_{ball} \quad (1)$$

$$SRR = 2 \cdot \frac{|(u_{disc} - u_{ball})|}{(u_{disc} + u_{ball})} \times 100\% \quad (2)$$

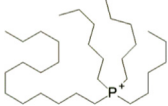
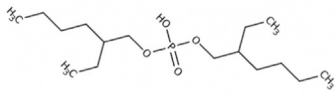
The reciprocating friction and wear tests of all the lubricant samples were performed in a CETR UMT-3 tribometer. The specimens used in these tribological tests are both manufactured from AISI 52100 steel and have the following main properties: ball (6 mm-diameter, 58–66 HRC of hardness, and 0.05 μm Ra of surface roughness) and disc (10 mm-diameter, 190–210 HV<sub>30</sub> of hardness, and 0.018 μm Ra of surface roughness). The lubricant volume used was 0.6 mL and test conditions were: 15 Hz of frequency, 4 mm of stroke length, 60 min-duration, temperature of 100 °C and loads of 5, 10, 15, 20 and 30 N (corresponding to maximum contact pressures of 1.13, 1.43, 1.63, 1.8 and 2.06 GPa). During the tribological tests the coefficient of friction (COF) was calculated and recorded, and each test was performed at least two times with a fresh lubricant sample resulting in a deviation lower than 1 %.

Before and after all tribological tests, the specimens were cleaned with heptane in an ultrasound bath for 10 min, rinsed in ethanol, and then dried with hot air.

### 2.4. Worn surface characterization

The disc wear volume was measured by confocal microscopy (Leica DCM 3D microscope). In addition, the wear mechanism and composition of the worn surface were analyzed by scanning

**Table 2**  
Physicochemical properties of the IL.

IL	Cation	Anion
Trihexyltetradecylphosphonium bis(2-ethylhexyl)phosphate [P <sub>6,6,6,14</sub> ][BEHP]	Trihexyltetradecylphosphonium	Bis(2-ethylhexyl)phosphate
Empirical formula: C <sub>48</sub> H <sub>102</sub> O <sub>4</sub> P <sub>2</sub> Purity: 98 % Molecular weight: 805.29		
Kinematic Viscosity at 40 °C (mm <sup>2</sup> /s)		528
Kinematic Viscosity at 100 °C (mm <sup>2</sup> /s)		59
Viscosity Index		181
Electrical Conductivity at 27 °C (μS/cm)		0.19

electron microscopy and energy dispersive spectroscopy (SEM/EDS), respectively, with a JEOL JSM-5600 equipment which operated at 15 and 20 kV. Later, the surface-lubricant chemical interaction was studied with a Raman confocal microscope (Model: WITec ALPHA300R+) using a laser with a wavenumber of 532 nm and a power in the range of 2.750–2.850 mW. A Zeiss EC Epiplan-Neofluar DIC Objective was used at 100x magnification. Spectra were taken in at least 6 points located at the central area of the wear scar. The number of accumulations for each spectrum was 100 and the integration period was 3 s.

### 3. Results and discussion

#### 3.1. Viscosity and electrical properties

Fig. 1 (left) shows how the  $\kappa$  of the ATF and its mixtures with the IL increased with temperature (due to the decrease of viscosity), which ease the migration of the charge carrier through the fluid. However, the  $\kappa$  of the ATF differs from that of the IL-containing mixtures even having similar viscosity, Fig. 1 (right). The [P<sub>6,6,6,14</sub>][BEHP] can be classified as a conductive compound considering its  $\kappa$  reported by Hernandez Battez et al. [18], meanwhile the ATF and the mixtures with the ionic liquid are dissipative fluids considering the classification of the ATFs depending on their  $\kappa$  found in Rodríguez et al. [17]. In addition, the ionicity of the ATF and its mixtures with the IL was evaluated through the Walden plot (Fig. 2), where the dotted line represents the so-called “good ionic” liquids. The results located far away from that line and at

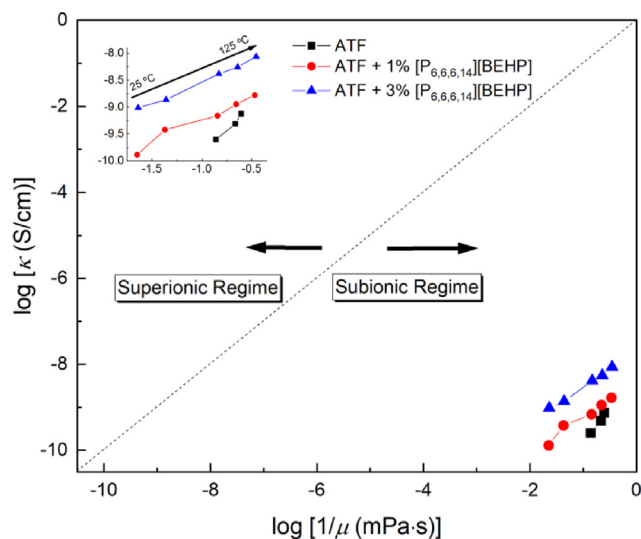


Fig. 2. Walden plot of the lubricant samples.

the lower side means that all the lubricant samples can be considered “non-ionic” liquids.

The differences in  $\kappa$  among the lubricant samples can be considered small because in general they do not exceed one order of magnitude. The dissipative and non-ionic characters of these ATF-IL mixtures are important from the perspective of the electric vehicle

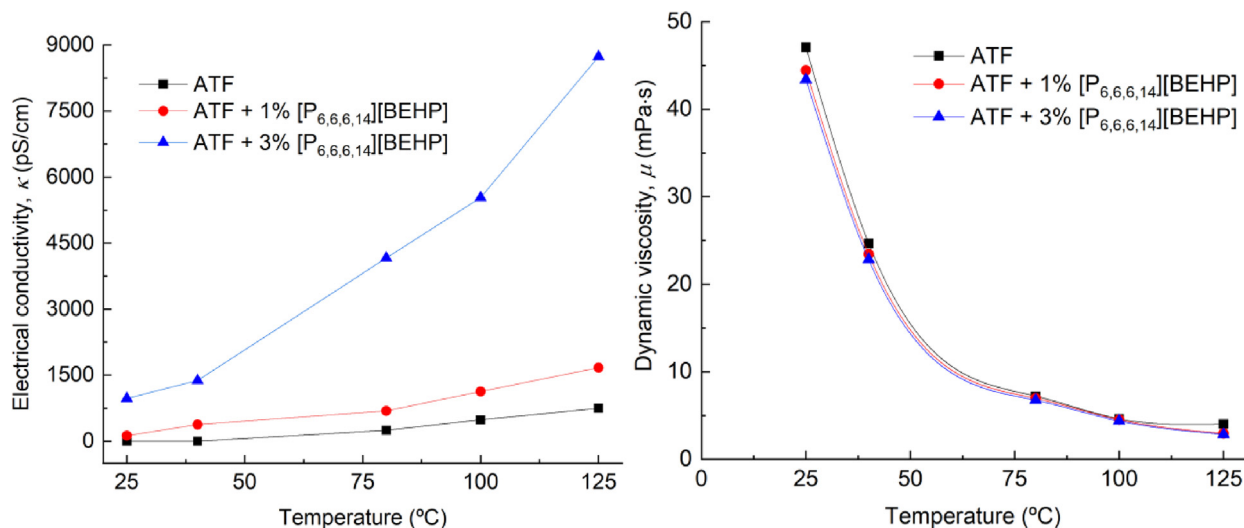


Fig. 1. Electrical conductivity and dynamic viscosity versus temperature of the lubricant samples.

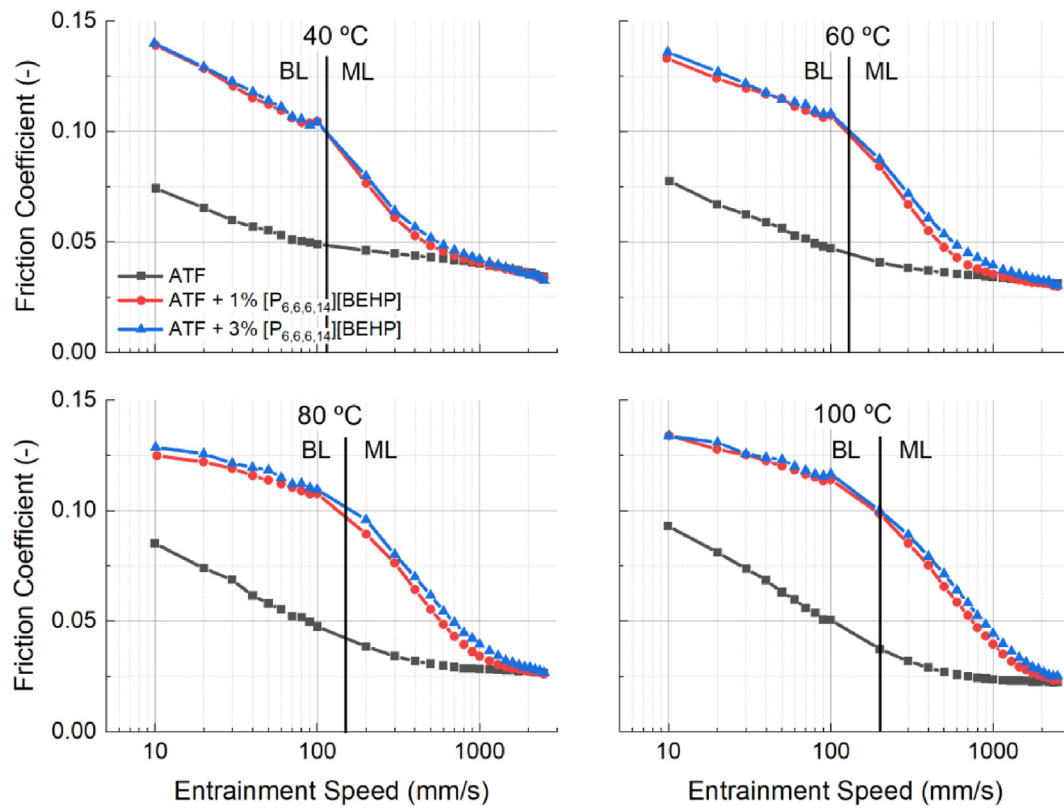


Fig. 3. Stribeck curves of the lubricant samples.

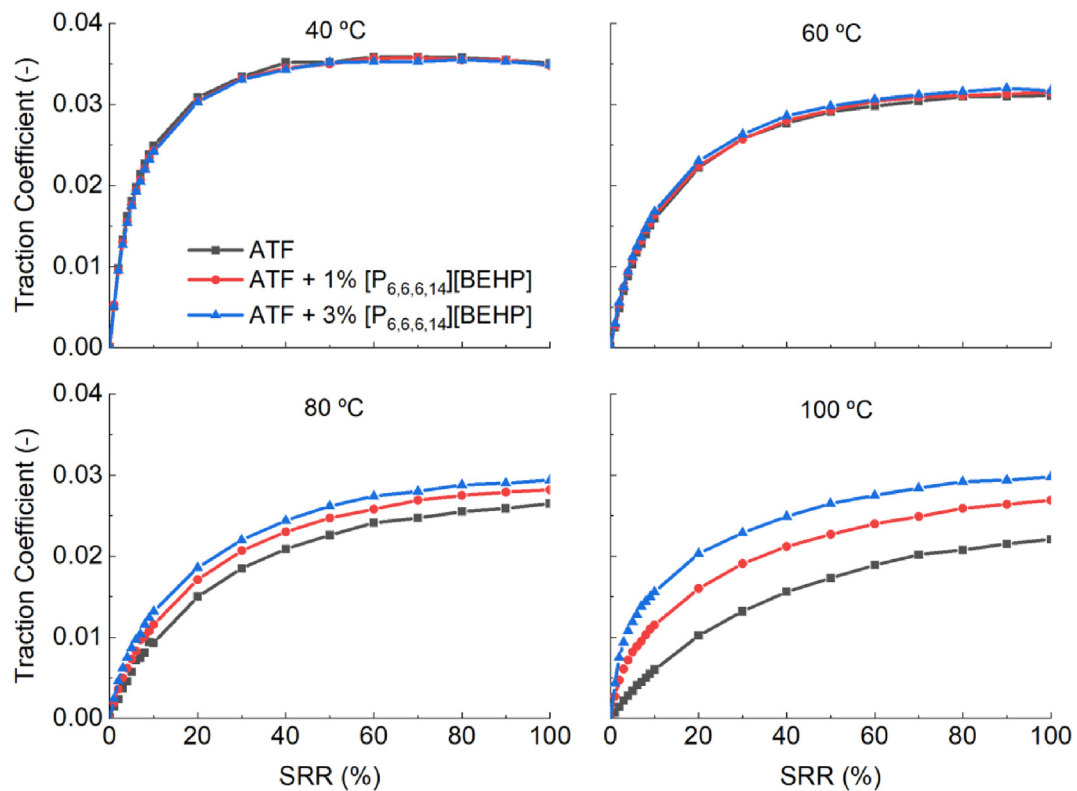


Fig. 4. Traction curves of the lubricant samples.

configuration incorporating the electric motor in the transmission housing.

Regarding the dielectric strength, the lubricant sample without IL showed a breakdown voltage of 46.2 kV for a water content of 164.2 ppm. However, it was not possible to determine this property in the remaining samples with a water content of 187.4 ppm and 219.4 ppm for the 1 % IL- and 3 % IL-containing samples, respectively. The presence of the IL could contribute to a higher water content and a huge decrease of dielectric breakdown voltage which is outside the detection limit of the test equipment. This great reduction of dielectric breakdown voltage due to the presence of impurities such as water or lubricant additives was also reported by Chen et al. [19]. However, even considering this breakdown voltage reduction, the lubricant sample could still be suitable for EVs because the maximum voltage in this application is under 1 kV.

### 3.2. Tribological tests

The tribological tests at variable entrainment speeds shows that the lubricant samples led to a similar coefficient of friction at the highest speeds, which coincides with the elastohydrodynamic lubrication (EHL) regime, Fig. 3. The ionic liquid-containing mixtures began to show higher coefficient of friction at decreasing entrainment speeds. This increase of friction with the mixtures begins first at higher temperatures when the lubricant film thickness become thinner, and the asperities contact lead to the formation of a thicker tribofilm due to the addition of the ionic liquid.

This behaviour was explained by Spikes [20] regarding the action mechanism of ZDDP as an antiwear additive under mild-wear or mixed lubrication regime. The lubricant samples containing the ionic liquid performed mainly under mixed (ML) and boundary (BL) lubrication regimes; meanwhile, the lubricant sample without ionic liquid performed under ML regime. The friction coefficient value taken as indicative of changing from mixed to boundary

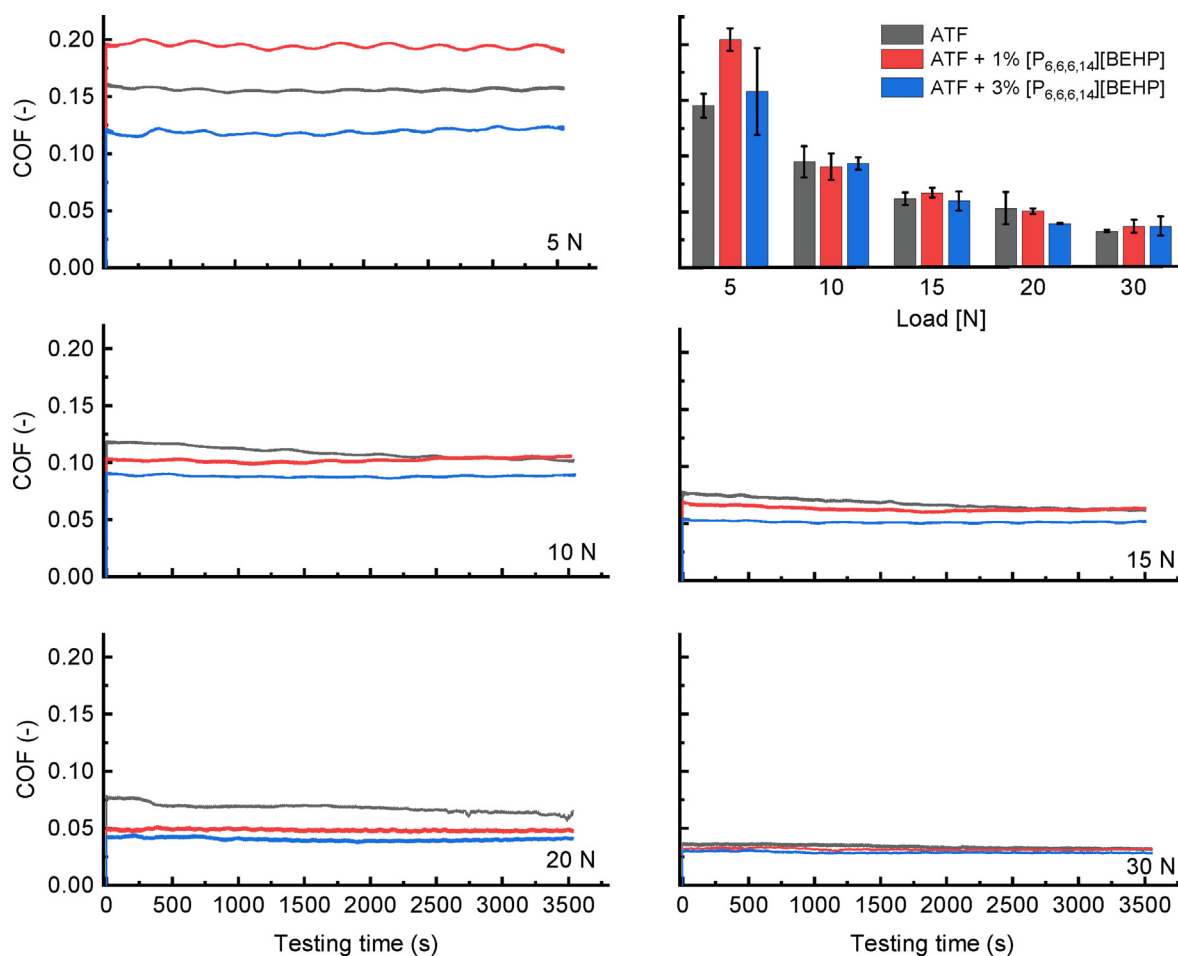


Fig. 5. Average COF and deviations during the reciprocating tests.

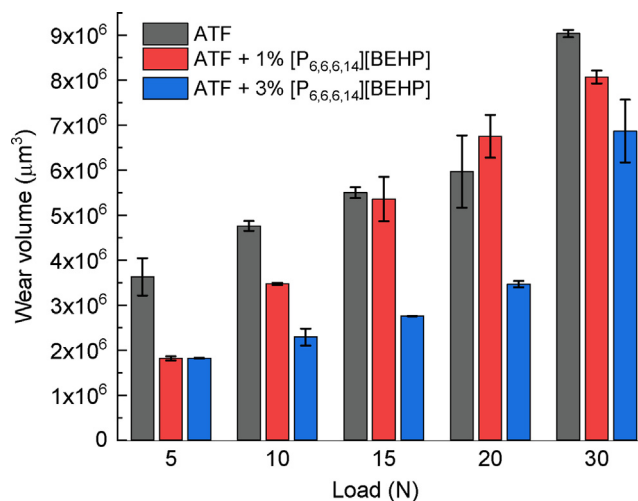


Fig. 6. Wear volume after the reciprocating tests.

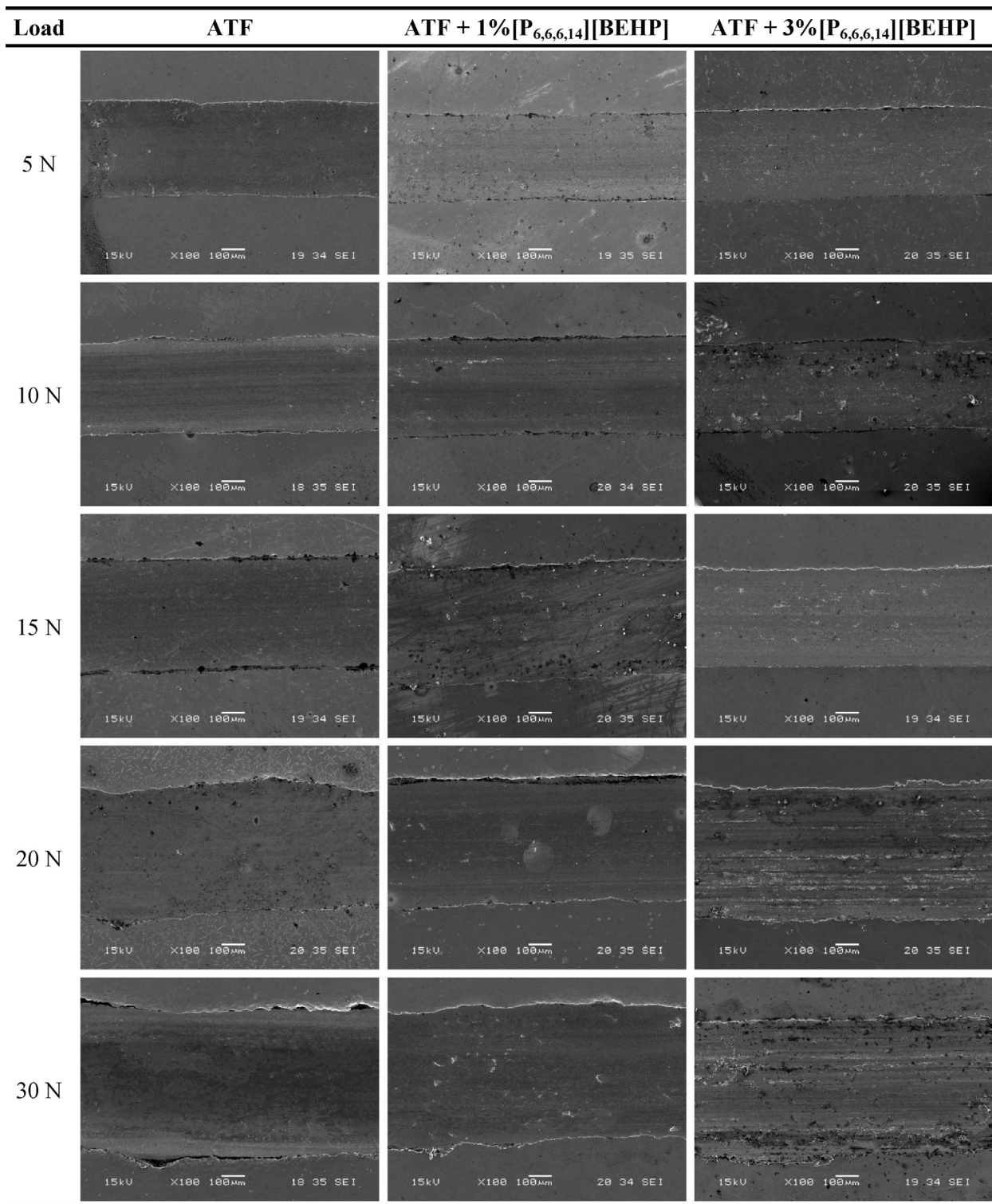


Fig. 7. SEM images of the worn surface after the friction and wear tests.

lubrication regime was 0.1. The higher friction values resulting from the tribofilm formed due to the presence of the IL are generally undesirable but is a sought-after characteristic for a fluid to be used in continuously variable transmissions [21].

The high entrainment speed, and the lower load and SRR values than in the Stribeck curve tests, lead the traction tests to be performed under elastohydrodynamic and hydrodynamic lubrication

conditions, Fig. 4. All the lubricant samples behaved similar at 40 and 60 °C because under these lubrication regimes (thicker lubricant films) friction is controlled by the lubricant viscosity, which is similar in all lubricant samples, Fig. 1. This no differentiation of the traction curves at low temperatures was also reported by Costello [22]. At higher temperatures (80 and 100 °C), friction was reduced because of the thinner lubricant film, and the differ-

entiation among the lubricant samples could be attributed to lower friction modifier content with the increase of the IL concentration.

Fig. 5 reports the average COF resulting of the reciprocating tests. In general, the friction values were similar for all the lubricant samples and a decreasing behaviour was observed at increasing loads. The decrease in friction with load below a friction coefficient value of 0.1, which is considered the virtual limit between the mixed and boundary lubrication regimes, could be connected to a stronger lubricant-surface chemical interaction due to a thinner lubricant film. The quick increase of friction under 5 N-load tests with the IL-containing lubricant samples could be related to the formation of an enhanced tribofilm due to the presence of the IL. This effect was no longer seen under higher loads probably because they also contributed to the wear of the tribofilm.

### 3.3. Worn surface characterization

On the contrary, the increasing load resulted in a higher wear for all the lubricant samples, Fig. 6. However, in general the addition of the IL reduced wear regarding the reference ATF, and its mixture containing 3 % of IL behaved better.

Fig. 7 shows the SEM images of the worn surface after the friction and wear tests and it can be observed that the wear mechanism was adhesive type. The wear increase with load was also verified through these images, as well as the plastic deformation at the edges of the wear scar.

Table 3 shows the EDS analysis of the worn surface on the discs and can be observed that the phosphorous concentration increased when the ionic liquids were added to the reference oil. The EDS technique has a depth of detection in order of microns, so the higher concentration of phosphorous found suggested the chemical interaction and the presence of this element on the worn surface. This fact was expected due to the P-containing cation and anion in the IL. Phosphorous also come from the typical antiwear additive ZDDP, which is prone to react with the metallic surface under mixed lubrication regime forming a boundary film. R. McDonald [23] analysed the tribofilm formation of P-containing antiwear and extreme pressure additives, ZDDPs in this case, and reported that this tribofilm is mainly formed by phosphates and can be as thinner as 20 nm and as thicker as 1  $\mu\text{m}$ . On the other hand, Qu et al. [13] reported that the ionic nature of the IL leads to a more efficient tribofilm formation than that of the ZDDP, resulting in a thicker tribofilm. When  $[\text{P}_{6,6,6,14}][\text{BEHP}] + \text{ZDDP}$  was used as antiwear additive in an engine oil, the tribofilm thickness formed was more than

the sum of the two formed separately. Considering this fact, the tribofilm thickness expected in the case of the ATF +  $[\text{P}_{6,6,6,14}][\text{BEHP}]$  could be greater than 1  $\mu\text{m}$  and be easily detected by the EDS as shown in Table 3.

When fully formulated oils (FFO) are used, the numerous additives included in their formulation can show either synergistic or antagonistic effects [12]. The addition of a P-containing ionic liquid to a FFO can lead to the formation polyphosphates of Fe, while the presence the ZDDP can result in the formation of a mixture polyphosphates, sulphates and sulphides of Zn/Fe in the tribofilm. In this case, the P and S found with the EDS technique suggest the formation of phosphate, sulphate and/or sulphide of Fe at the detection limit of this technique. However, higher concentration and other compounds can be detected on the surface by using other techniques (e.g. XPS, Raman, etc.).

Raman analyses, as shown in Fig. 8, revealed the presence of iron oxides in the wear scar. Particularly, a characteristic Fe-O ( $\text{Fe}_3\text{O}_4$ ) stretch vibration peak appears at approximately  $667\text{ cm}^{-1}$  [24–26] and at  $540\text{ cm}^{-1}$  [26] also, although with less intensity. In addition, characteristic peaks of  $\text{Fe}_2\text{O}_3$  are observed at 220, 290, 410, 613 and  $1318\text{ cm}^{-1}$  [24,26,27].

Raman spectra also show other several peaks in the  $100\text{--}530\text{ cm}^{-1}$  region.  $\text{PO}_2^-$  and  $\text{PO}_4^-$  bending vibration peaks were observed at 110, 126, 168, 442 and  $525\text{ cm}^{-1}$  [24,28]. Peaks at 220 and  $272\text{ cm}^{-1}$  are assigned to Fe-S vibrations and various polysulfide species [29]. S–S stretching peaks at  $460\text{--}480\text{ cm}^{-1}$  and a Zn-S peak at  $350\text{ cm}^{-1}$  were also observed [24]. Likewise, in almost all the spectra two characteristic peaks appear at  $1340\text{ cm}^{-1}$  and  $1580\text{ cm}^{-1}$  corresponding to the D and G bands of carbon materials [25,30]. The asymmetry in the intensities of the D and G bands of the spectra, as well as the width of the peaks, suggests that the carbon analyzed in the wear scar is structurally amorphous graphite [27].

On the other hand, in the  $930\text{--}1100\text{ cm}^{-1}$  spectral region, most of the peaks are assigned to phosphate compounds [31] (mainly iron polyphosphates [28,32] and Zn polyphosphates [26,32]). In addition, the lower intensity peaks that appear at 1020, 1090 and  $1195\text{ cm}^{-1}$  are assigned to sulphate compounds (mainly  $\text{ZnSO}_4$ ) [33].

As can be seen in the Raman spectra (Fig. 8), the peaks assigned to phosphorus compounds located in the spectral regions  $100\text{--}530\text{ cm}^{-1}$  (bending vibration peaks) and  $930\text{--}1100\text{ cm}^{-1}$  (stretching vibration peaks) increase considerably its intensity when the concentration of the IL is higher. These results are in agreement with the higher concentration of phosphorus that is also observed in the EDS analysis when increasing the concentration of IL, and for all loads (Table 3). This suggests that the addition of IL improves

**Table 3**  
EDS analysis from the wear scar on the disc.

Oil	Load (N)	Concentration of chemical elements (wt%)							
		C	O	Si	P	S	Cr	Mn	Fe
ATF	5	7.43	10.03	0.19	0.04	0.83	3.02	0.83	77.64
	10	6.82	10.43	0.16	0	0.73	2.91	0.64	78.25
	15	6.95	11.83	0.38	0.02	0.88	2.17	0.51	77.26
	20	6.99	12.08	0.10	0.06	1.54	4.20	0.74	74.09
	30	6.97	11.35	0.18	0.20	1.30	3.11	0.58	76.17
ATF + 1 % IL	5	7.13	10.70	0.12	0.46	0.21	0.73	0.65	77.89
	10	6.70	11.86	0.20	0.58	0.47	2.94	0.59	76.57
	15	6.90	12.86	0.28	0.27	0.49	2.11	0.30	76.68
	20	7.13	13.65	0.21	0.31	0.50	1.93	0.59	75.48
	30	6.67	11.45	0.36	0.32	0.57	2.37	0.50	77.69
ATF + 3 % IL	5	6.77	10.72	0.29	0.48	0.30	2.51	0.64	78.07
	10	7.14	11.07	0.11	0.61	0.26	2.85	0.53	77.39
	15	8.44	10.35	0.23	0.54	0.19	2.76	0.47	76.95
	20	7.34	11.60	0.22	0.49	0.28	2.22	0.56	77.29
	30	6.94	10.41	0.24	0.88	0.12	2.27	0.57	78.48

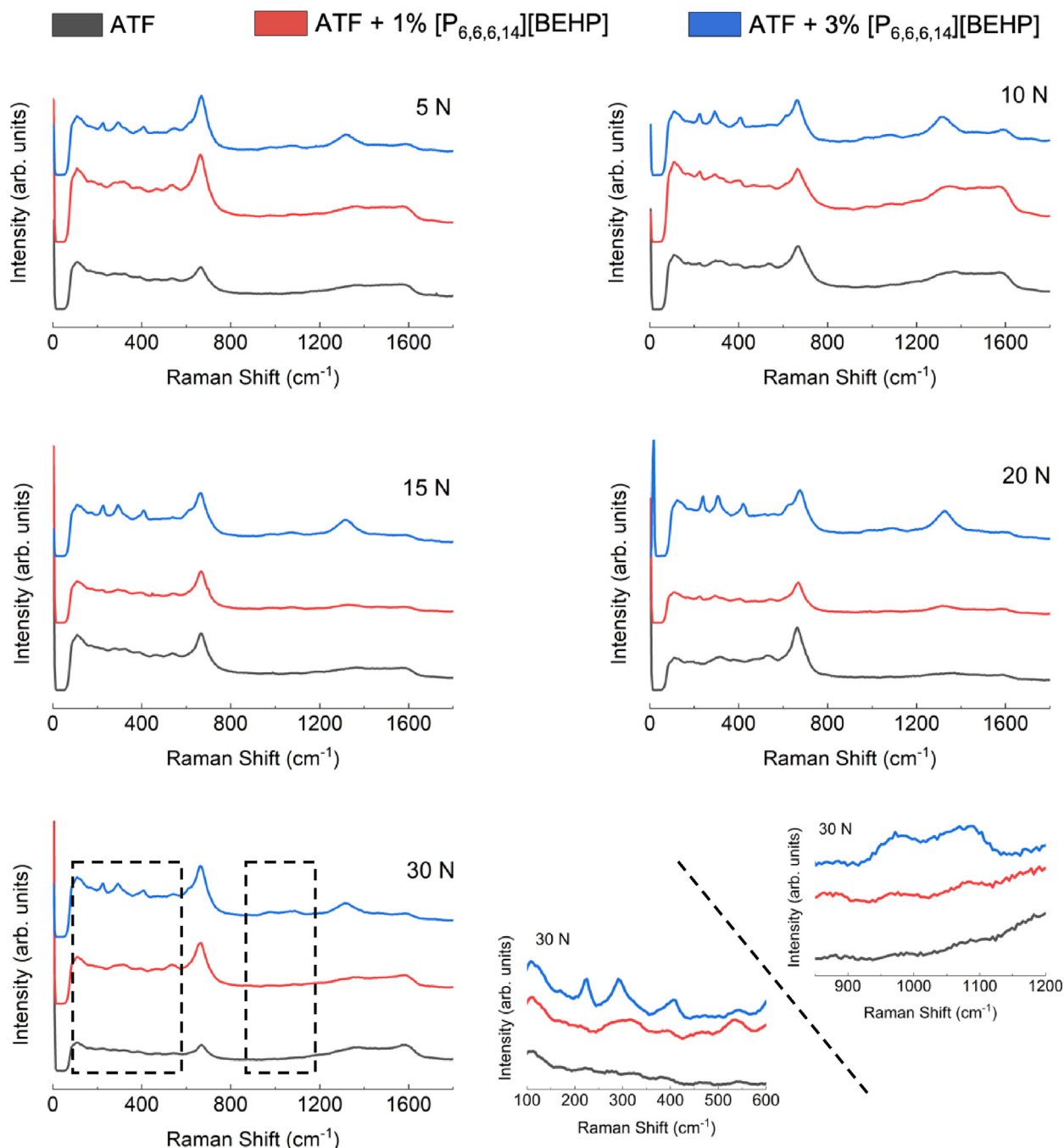


Fig. 8. Raman spectra from wear scar after friction and wear tests.

the kinetics of the phosphorus-enriched tribofilm formation, which acts as a protective film against wear [32].

#### 4. Conclusions

The electrical compatibility, as well as improved tribological behaviour, are important requirements for the ATFs to be used in electrical vehicles which include the electric motor in the transmission housing. Both requirements are dependent on the additive type and concentration. The use of ionic liquids has been recommended as conductivity agents in the formulation of ATFs but they also affect tribological behaviour. The influence of the addition of the trihexyltetradecylphosphonium bis(2-ethylhexyl)

phosphate ( $[P_{6,6,6,14}][BEHP]$ ) ionic liquid on the  $\kappa$  and tribological behaviour of a fully-formulated ATF was studied in this work.

From the obtained results can be drawn the following conclusions:

- The addition of the ionic liquid did not change the “non-ionic” property of the ATF and it remains being classified as dissipative; however, the dielectric strength decreased drastically and further tests about this property should be performed.
- The presence of the IL increased traction probably due to the decrease of the friction modifier content with the increase of the IL concentration and the thinner lubricant film at higher temperatures.



- The tribofilm formation hardly changed friction under pure sliding motion but decreased wear, outperforming the tribological behavior of the commercial ATF used as reference oil.

### CRedit authorship contribution statement

**A. García Tuero:** Investigation, Validation, Writing – original draft, Writing – review & editing. **C. Sanjurjo:** Investigation, Writing – original draft. **N. Rivera:** Investigation, Methodology, Writing – original draft, Writing – review & editing. **J.L. Viesca:** Conceptualization, Investigation, Writing – original draft, Project administration. **R. González:** Supervision, Methodology, Writing – review & editing. **A. Hernández Battez:** Methodology, Supervision, Validation, Project administration, Writing – original draft, Writing – review & editing.

### Data availability

Data will be made available on request.

### Declaration of Competing Interest

The authors declare that they have no known competing financial interests or personal relationships that could have appeared to influence the work reported in this paper.

### Acknowledgments

The authors would like to acknowledge the Ministry of Science, Innovation and Universities (Spain) for supporting this work under the project PID2019-109367RB-100. Authors would like to thank the use of the RIAIDT facilities (University of Santiago de Compostela, Spain), in particular to Mr. Ezequiel Vázquez.

### References

- [1] M. Woydt, The importance of tribology for reducing CO<sub>2</sub> emissions and for sustainability, *Wear* 474–475 (2021) 203768, <https://doi.org/10.1016/j.wear.2021.203768>.
- [2] Lubes'n'Greases Perspective on Electric Vehicles Annual Report, LNG Publishing Company, Inc., 2019, pp. 23–27.
- [3] L.I. Farfan-Cabrera, Tribology of electric vehicles: a review of critical components, current state and future improvement trends, *Tribol. Int.* 138 (2019) 473–486, <https://doi.org/10.1016/j.triboint.2019.06.029>.
- [4] A. Gangopadhyay, P.D. Hanumalagutti, Challenges and opportunities with lubricants for HEV/EV vehicles, in: Proceedings of the STLE Annual Meeting & Exhibition, Nashville, TN, USA, 19–23 May 2019.
- [5] Z. Gao, L. Salvi, S. Flores-Torres, High conductivity lubricating oils for electric and hybrid vehicles, Patent US 2018/0100115 A1. ExxonMobil Research and Engineering Co.
- [6] C. Ye, W. Liu, Y. Chen, L. Yu, Room-temperature ionic liquids: a novel versatile lubricant, *Chem. Commun.* 21 (21) (2001) 2244–2245, <https://doi.org/10.1039/B106935G>.
- [7] F. Zhou, Y. Liang, W. Liu, Ionic liquid lubricants: designed chemistry for engineering applications, *Chem. Soc. Rev.* 38 (9) (2009) 2590–2599, <https://doi.org/10.1039/B817899M>.
- [8] M.D. Bermúdez, A.E. Jiménez, J. Sanes, F.J. Carrión, Ionic liquids as advanced lubricant fluids, *Molecules* 14 (8) (2009) 2888–2908, <https://doi.org/10.3390/molecules14082888>.
- [9] I. Minami, Ionic liquids in tribology, *Molecules* 14 (6) (2009) 2286–2305, <https://doi.org/10.3390/molecules14062286>.
- [10] Y. Zhou, J. Qu, Ionic liquids as lubricant additives: a review, *ACS Appl. Mater. Interf.* 9 (4) (2017) 3209–3222, <https://doi.org/10.1021/acsami.6b12489>.
- [11] J. Qu, H. Luo, M. Chi, C. Ma, P.J. Blau, S. Dai, M.B. Viola, Comparison of an oil-miscible ionic liquid and ZDDP as a lubricant anti-wear additive, *Trib. Int.* 71 (2014) 88–97, <https://doi.org/10.1016/j.triboint.2013.11.010>.
- [12] J. Qu, W.C. Barnhill, H. Luo, H.M. Meyer III, D.N. Leonard, A.K. Landauer, B. Kheireddin, H. Gao, B.L. Papke, S. Dai, Synergistic effects between phosphonium-alkylphosphate ionic liquids and zinc dialkyldithiophosphate (ZDDP) as lubricant additives, *Adv. Mater.* 27 (2015) 4767–4774, <https://doi.org/10.1002/adma.201502037>.
- [13] J. Qu, D.G. Bansal, B.o. Yu, J.Y. Howe, H. Luo, S. Dai, H. Li, P.J. Blau, B.G. Bunting, G. Mordukhovich, D.J. Smolenski, Antiwear performance and mechanism of an oil-miscible ionic liquid as a lubricant additive, *ACS Appl. Mater. Interf.* 4 (2) (2012) 997–1002.
- [14] R. Monge, R. González, A. Hernández Battez, A. Fernández-González, J.L. Viesca, A. García, M. Hadfield, Ionic liquids as an additive in fully formulated wind turbine gearbox oils, *Wear* 328–329 (2015) 50–63, <https://doi.org/10.1016/j.wear.2015.01.041>.
- [15] C.M.C.G. Fernandes, A. Hernandez Battez, R. González, R. Monge, J.L. Viesca, A. García, R.C. Martins, J.H.O. Seabra, Torque loss and wear of FZG gears lubricated with wind turbine gear oils using an ionic liquid as additive, *Tribol. Int.* 90 (2015) 306–314, <https://doi.org/10.1016/j.triboint.2015.04.037>.
- [16] S. Flores-Torres, D.G.L. Holt, J.T. Carey, Method for Preventing or Minimizing Electrostatic Discharge and Dielectric Breakdown in Electric Vehicle Powertrains. WO/2018/067905.
- [17] E. Rodríguez, N. Rivera, A. Fernández-González, T. Pérez, R. González, A. Hernández Battez, Electrical compatibility of transmission fluids in electric vehicles, *Trib. Int.* 171 (2022) 107544, <https://doi.org/10.1016/j.triboint.2022.107544>.
- [18] A. Hernández Battez, M. Bartolomé, D. Blanco, J.L. Viesca, A. Fernández-González, R. González, Phosphonium cation-based ionic liquids as neat lubricants: physicochemical and tribological performance, *Trib. Int.* 95 (2016) 118–131, <https://doi.org/10.1016/j.triboint.2015.11.015>.
- [19] Y. Chen, S. Jha, A. Raut, W. Zhang, H. Liang, Performance characteristics of lubricants in electric and hybrid vehicles: a review of current and future needs, *Front. Mech. Eng.* 6 (2020) 571464, <https://doi.org/10.3389/fmech.2020.571464>.
- [20] H. Spikes, The history and mechanisms of ZDDP, *Trib. Lett.* 17 (2004) 469–489, <https://doi.org/10.1023/B:TRIL.0000044495.26882.b5>.
- [21] M. Kano, Y. Mabuchi, T. Ishikawa, A. Sano, T. Wakizono, The effect of ZDDP in CVT fluid on increasing the traction capacity of belt-drive continuously variable transmissions, *Lub. Sc.* 11 (4) (1999) 365–377.
- [22] M.T. Costello, Effects of basestock and additive chemistry on traction testing, *Trib. Lett.* 18 (2005) 91–97, <https://doi.org/10.1007/s11249-004-1761-z>.
- [23] R. McDonald, Zinc Dithiophosphates, in: *Lubricant Additives: Chemistry and Applications*, L.R. Rudnick, second ed., CRC Press, 2009, pp. 51–69.
- [24] H. Okubo, C. Tadokoro, S. Sasaki, In situ Raman-SLIM monitoring for the formation processes of MoDTC and ZDDP tribofilms at steel/steel contacts under boundary lubrication, *Tribol. Online* 15 (3) (2020) 105–116, <https://doi.org/10.2474/TROL.15.105>.
- [25] B. Wang, Z. Zhong, H. Qiu, D. Chen, W. Li, S. Li, X. Tu, Nano serpentine powders as lubricant additive: tribological behaviors and self-repairing performance on worn surface, *Nanomaterials* 10 (2020) 922, <https://doi.org/10.3390/nano10050922>.
- [26] A. Dorgham, A. Azam, P. Parsaeian, C. Wang, A. Morina, A. Neville, An assessment of the effect of relative humidity on the decomposition of the ZDDP antiwear additive, *Trib. Lett.* 69 (2021) 72, <https://doi.org/10.1007/s11249-021-01446-6>.
- [27] A. Erdemir, G. Ramirez, O.L. Eryilmaz, B. Narayanan, Y. Liao, G. Kamath, S.K.R.S. Sankaranarayanan, Carbon-based tribofilms from lubricating oils, *Nature* 536 (2016) 67–71, <https://doi.org/10.1038/nature18948>.
- [28] M.P. Pasternak, G.K. Rozenberg, A.P. Milner, M. Amanowicz, T. Zhou, U. Schwarz, K. Syassen, R.D. Taylor, M. Hanfland, K. Brister, Pressure-induced concurrent transformation to an amorphous and crystalline phase in berlinite-type FePO<sub>4</sub>, *Phys. Rev. Lett.* 79 (22) (1997) 4409–4412, <https://doi.org/10.1103/PhysRevLett.79.4409>.
- [29] A. Matamoros-Veloza, O. Cespedes, B.R.G. Johnson, T.M. Stawski, U. Terranova, N.H. Leeuw, L.G. Benning, A highly reactive precursor in the iron sulfide system, *Nat. Commun.* 9 (2018) 3125, <https://doi.org/10.1038/s41467-018-05493-x>.
- [30] Z. Wang, C. Liu, G. Shi, G. Wang, H. Zhang, Q. Zhang, X. Jiang, X. Li, F. Luo, Y. Hu, K. Yi, Preparation and electrochemical properties of electrospun FeS/carbon nanofiber composites, *Ionics* 26 (2020) 3051–3060, <https://doi.org/10.1007/s11581-020-03455-2>.
- [31] Infrared and Raman Characteristic Group Frequencies. Tables and Charts. Third Ed. George Socrates. John Wiley & Sons, LTD.
- [32] V. Sharma, C. Gabler, N. Doerr, P. Aswath, Mechanism of tribofilm formation with P and S containing ionic liquids, *Trib. Int.* 92 (2015) 353–364, <https://doi.org/10.1016/j.triboint.2015.07.009>.
- [33] SpectraBase. <<https://spectrabase.com/spectrum/8wfgtjvmAH>>.